



Integrity testing of Planova™ BioEX virus removal filters used in the manufacture of biological products



Shinya Sekine ^a, Masayasu Komuro ^b, Takayuki Sohka ^{c,*}, Terry Sato ^c

^a Bioprocess Technology Development Department, Asahi Kasei Medical MT Corporation, 5-4960 Nakagawara, Nobeoka, Miyazaki 882-0031, Japan

^b Medical Material Laboratory, Medical Products Development Division, Asahi Kasei Medical Co., Ltd., 5-4960 Nakagawara, Nobeoka, Miyazaki 882-0031, Japan

^c Technical Marketing Department, Bioprocess Division, Asahi Kasei Medical Co., Ltd., 1-105 Kanda Jinbocho, Chiyoda-ku, Tokyo 101-8101, Japan

ARTICLE INFO

Article history:

Received 25 August 2014

Received in revised form

7 February 2015

Accepted 9 February 2015

Available online 7 March 2015

Keywords:

Planova™ BioEX virus filter

Air/water diffusion-based leakage test

Integrity testing

Forward/diffusive flow

Biologicals

ABSTRACT

Confirmation of virus filter integrity is crucial for ensuring the safety of biological products. Two main types of virus filter defects may produce inconsistent and undesirable performance in virus removal: improper pore-size distribution across the membrane; and specific damage, such as tears, broken fibers, or pinholes. Two integrity tests are performed on each individual filter manufactured by Asahi Kasei Medical to ensure the absence of these defects prior to shipment. In this study, we verified that typical usage of Planova™ BioEX filters would not improperly shift the pore-size distribution. Damage occurring during shipment and use (e.g., broken fibers or pinholes) can be detected by end-users with sufficient sensitivity using air–water diffusion based leakage tests. We prepared and tested filters with model pinhole defects of various sizes to develop standard acceptance criteria for the leakage test relative to porcine parvovirus infectivity logarithmic reduction values (LRVs). Our results demonstrate that pinhole defects at or below a certain size for each effective filter surface area have no significant impact on the virus LRV. In conclusion the leakage test is sufficiently sensitive to serve as the sole end-user integrity test for Planova™ BioEX filters, facilitating their use in biopharmaceuticals manufacturing.

© 2015 Asahi Kasei Medical CO., LTD. Published by Elsevier Ltd on behalf of The International Alliance for Biological Standardization. This is an open access article under the CC BY-NC-ND license (<http://creativecommons.org/licenses/by-nc-nd/4.0/>).

1. Introduction

Fractionated plasma products and biopharmaceuticals, such as recombinant proteins and monoclonal antibodies, are playing an increasingly important role in human medicine [1,2]. However, the starting material for these products carries the risk of contamination by viruses and other pathogens. In order to ensure patient safety, regulations and guidelines for removing viruses have been enacted and proposals have been made for the implementation and validation of virus removal and inactivation methods [3–8]. The respective strengths and limitations of various virus inactivation and removal methods have been the subjects to continuous discussion among both regulators and manufacturers of

Abbreviations: BP, bubble point; GPT, gold particle test; IT, integrity test; LRV, logarithmic reduction value; Lv, leak value; PLT, Planova™ Leak Tester; PPV, porcine parvovirus; PVDF, polyvinylidene fluoride; SD, standard deviation; TCID₅₀, 50% tissue culture infectious dose.

* Corresponding author. Tel.: +81 3 3296 3783.

E-mail address: souka.tb@om.asahi-kasei.co.jp (T. Sohka).

<http://dx.doi.org/10.1016/j.biologicals.2015.02.003>

1045-1056/© 2015 Asahi Kasei Medical CO., LTD. Published by Elsevier Ltd on behalf of The International Alliance for Biological Standardization. This is an open access article under the CC BY-NC-ND license (<http://creativecommons.org/licenses/by-nc-nd/4.0/>).

biopharmaceuticals in the last few years. Virus filtration, also known as nanofiltration, is a gentle, nonspecific, and widely applied process that removes virus particles from solutions based on size exclusion properties that do not alter the functional and antigenic characteristics of most proteins [9–12]. Planova™ BioEX filters (manufactured by Asahi Kasei Medical, Co., Ltd., Japan) are composed of membranes of hollow fibers made of hydrophilic modified polyvinylidene fluoride (PVDF). PVDF is used to produce membranes for ultrafiltration [13], nanofiltration [14], and hemodialysis and is recognized for its mechanical strength [15].

Performing integrity tests (ITs) on virus filters both before and after nanofiltration is very important for confirming filter integrity and for supporting claims of virus removal. Several IT methods have been developed for virus filters [10,11,16–19]. For example, in the case of Planova™ cellulose filters, a post-use test using gold colloid particles can be used to assess improper shifts in membrane pore-size distribution. Although highly effective, this gold particle test (GPT) has the drawback of being destructive, and therefore, it cannot be performed prior to using the filter in the process setting. Thus, other testing strategies that are both accurate in assessing

membrane pore-size distribution and are efficient, robust, and user friendly must be considered.

Virus filters are verified as having the specified pore-size distribution and to be free from other defects before shipment to end-users. Several pore-size distribution ITs, such as the bubble point (BP) method, are conducted through routine sampling during the spinning of hollow-fiber membranes. In addition, each Planova™ BioEX filter is subjected to a pressure hold test and a leakage test [10,16]. End-user ITs conducted before use of the filter in the process stream must be non-destructive and should not require specialized solutions or set-up that would compromise the quality of the biopharmaceutical product or be difficult to perform. ITs for detecting improper shifts in pore-size distribution may not be required if the filter has physical and chemical properties that are sufficiently robust to withstand the filtration conditions used. On the other hand, any damage occurring during shipment and use is likely to result in gross defects larger than the micron scale, including hollow fiber breakage. Pre- and post-use ITs performed by the end-user are needed to detect such damage. Typical large gross defects should be easily detectable by visual inspection; however, it is also important to consider the risk of hard-to-detect defects that may impact virus retention capacity.

Many approaches exist for detecting the presence of post-shipment gross defects. Methods using particles and bacteria to detect artificially produced and actual defects in the micrometer-scale range in ultrafiltration membranes have been reported [20,21]. For virus removal filters, original and modified leakage tests based on air–water diffusion are commonly used and regularly evaluated [10,16,19]. Methods involving binary gases and water/organic solvent mixtures have also been developed [22–24]. The approach we follow, known as the “single-point forward/diffusive flow test” [10,16,19], is relatively simple and can be used to detect micrometer-size gross defects.

In this report, we demonstrate the resistance of Planova™ BioEX filters to improper shifts in pore-size distribution and the maintenance of virus removal capacity even after harsh conditionings. We also discuss the use of an air/water diffusion–based leakage test as an IT for detecting gross defects associated with pinhole damage to the membrane, and we demonstrate the relationship between pinhole size and detection using air/water diffusion-based leakage tests and virus removal. Finally, the use of the leakage test as the only end-user IT for Planova™ BioEX filters is discussed.

2. Material and methods

2.1. Harsh conditioning of Planova™ BioEX filters

Planova™ BioEX (0.001 m² or 0.01 m²) filters were conditioned by filtering 1000-mL solutions of either low pH (pH 2: hydrochloric acid aqueous solution) or high pH (pH 10: sodium hydroxide aqueous solution) at high temperature (40 °C) under a filtration pressure of 392 kPa (3.92 bar, 56.9 psi) for 12 h (the solution was recirculated and filtered multiple times during the experimental period), after which the filter was flushed with an excess of purified water (100 L/m²). Control filters were used without any of the harsh conditioning described above.

In this report, all pressures are indicated as the filter inlet gauge pressure (above ambient atmospheric pressure), and the permeate side would have ambient atmospheric pressure only.

2.2. Virus propagation and virus removal study

Porcine parvovirus (PPV, 90HS strain, Japanese Association of Veterinary Biologics, Tokyo, Japan) was propagated in PK-13 cells (ATCC #CRL-6489) at 37 °C in Dulbecco's modified Eagle's medium

(DMEM) supplemented with 3% (v/v) fetal bovine serum. At first sign of the death of inoculated host cells, the medium was exchanged with serum-free DMEM. The supernatant (containing a high titer of serum-free PPV) was collected, centrifuged at 1710 × g for 20 min at 4 °C, and then filtered through a 0.45-µm filter to remove the cell debris. This virus stock was titrated and stored at –80 °C until use [25,26].

The PPV stock was spiked into human polyclonal IgG (Venoglobulin®-IH, Japan Blood Products Organization, Japan). For harshly conditioned filters (0.001 m²), the final virus-load sample was comprised of 0.5% (v/v) PPV stock suspension in 30 mg/mL human IgG/0.1 M sodium chloride aqueous solution. For pinhole filters, the final virus-load sample was comprised of 0.5% (v/v) PPV stock suspension in 30 or 1 mg/mL human IgG/0.1 M sodium chloride aqueous solution. Due to experimental limitations, the experiments using filters with a large effective surface area (1.0, 4.0, and 0.1 m²) were conducted at the lower human IgG concentration, whereas tests of filters with 0.1-m² pinholes were conducted at both IgG concentrations and analyzed as a series of experiments. As a clear relationship between virus removal rate and a pinhole size of 0.1 m² was observed at both IgG concentrations, it was determined that protein concentration does not affect the virus removal rate and filtration flux.

After pre-filtration with Planova™ 35N filters (Asahi Kasei Medical, Ltd.) at 50 kPa (0.50 bar, 7.3 psi) for the purpose of obtaining mono-dispersed PPV particles, virus filtration experiments were conducted under 196-kPa (1.96 bar, 28.4 psi) dead-end, constant-pressure filtration at 25 °C. The virus titer was determined by hemagglutinin assay and was quantified as the 50% tissue culture infectious dose (TCID₅₀), determined by the method of Reed and Muench using PK-13 cells [27]. For the harshly conditioned filters (0.001 m²), the initial titer of the virus load solution (after pre-filtration with Planova™ 35N) was set between 10^{5.7} and 10^{6.0} TCID₅₀/mL, and the filtration volume was 105 L/m², with permeate collection for analysis at the 100–105 L/m² fraction. For the pinhole filters (0.1, 1.0, and 4.0 m²), the initial virus titer of the virus load solution (after pre-filtration with Planova™ 35N) was set to 10^{6.2}, 10^{6.0}, or 10^{6.7} TCID₅₀/mL, and the filtration volume was 5 L/m², with permeate collection for analysis at the 2–3 L/m² fraction. The TCID₅₀ was measured using the same method. Virus (PPV) removability was expressed as the logarithmic reduction value (LRV), or PPV LRV.

2.3. Gold particle test

Harshly conditioned Planova™ BioEX (0.01 m²) filters and control filters receiving no pretreatment were subjected to the GPT [28,29]. Test solution containing colloidal gold particles (diameter of approximately 20 nm; Asahi Kasei Medical, Ltd.) was prepared as directed and filtered using 98-kPa (0.98 bar, 14.2 psi) dead-end constant-pressure filtration at 25 °C. The filtration volume was 1.0 L/m², and the permeate (0.5–1.0 L/m² fraction) was collected and the absorbance was assayed at 530 nm (UV–VIS spectrophotometer, UV2450, Shimadzu, Japan). Gold particle removability was expressed as LRV.

2.4. Model pinhole filters

A krypton fluoride (KrF) excimer laser was used to make single pinholes in individual fibers, and this work was performed by L.P.S. Works Co., Ltd. (Tokyo, Japan). Briefly, a Planova™ BioEX hollow fiber was positioned such that irradiation by the KrF excimer laser would penetrate through one surface of the BioEX hollow fiber and produce a single pinhole. Each pinhole fiber was then crafted into a filter of 0.001 or 0.01 m² effective surface area using normal hollow

fibers to complete the filters. For pinhole filters with an effective surface area of 0.1, 1.0, and 4.0 m², the pinhole fiber was set deep in the normal hollow-fiber bundle and crafted into the filter. The presence of only one single-pinhole fiber in each filter was assured during the assembly step of the filter.

After finishing a series of flow-rate tests, the hollow fibers from a subset of filters with an effective surface area of 0.1 m² or smaller were recovered from the pinhole filter and the pinhole fiber was identified. The pinhole was observed under a scanning electron microscope (Fig. 1a), and the diameter of the pinhole was measured. The pinhole was smaller on the inner surface of the hollow fiber. Therefore, in this paper, the “pinhole diameter” is taken to be the diameter of the pinhole on the inner surface, as depicted in Fig. 1b. The relationship between pinhole size, leak value, and PPV LRV was then determined.

2.5. Pinhole size determination based on the water overflow rate

In this section, we explain the pinhole associated water overflow rate and discuss it together with the critical flow model equation. The appropriateness is examined further in the Discussion section.

We used water overflowing from the filter permeate side outlet nozzle as a surrogate for airflow across hollow-fiber membranes with normal pores and pinhole defects. The airflow volume across the membrane displaces a proportional volume of water on the filter permeate side. Therefore, the water overflow rate was used to obtain data to estimate the size of the pinhole defect.

The permeate side of the filter was filled with air-saturated water at 25 °C under ambient atmospheric pressure, and then compressed air was applied to the feed side of the filter at 343 kPa (3.43 bar, 49.7 psi). After a stabilization period, the water overflow rate was measured. The water overflow rate was determined for both normal-pore and pinhole-containing filters, and the difference was taken as the flow attributable to the pinhole.

The actual data were proportional to the pinhole radius square. Thus, the data were modeled using the following methods. The

maximum-weight air flow rate from a single pinhole defect, W_{\max} , is described by Eq. (1) (adapted from Ref. [30], section 10–19 “Critical flow nozzle” for air: equation (10–33)). The application of this equation will be addressed in more detail in the Discussion section.

$$W_{\max} = C_1 C A_2 p_1 / \sqrt{T_1} \quad (1)$$

where C_1 represents the dimensional constant; C represents the coefficient of discharge (dimensionless; discharge coefficient for critical flow nozzles in general, the same as that for subsonic nozzles [30]); A_2 represents the cross-sectional area of the pinhole; p_1 represents the absolute pressure inside the hollow fiber; T_1 represents the absolute temperature in the hollow fiber; and W_{\max} represents the maximum-weight airflow rate (kg/min).

By holding the experimental conditions constant at 343 kPa (gauge pressure; 3.43 bar, 49.7 psi) and 25 °C, W_{\max} can be converted to the volumetric airflow rate, Q_{air} (mL/min) at 25 °C under ambient atmospheric pressure. Likewise, the constants C_1 and C along with the square root of T_1 can be reduced to a constant. Our experimentally created pinhole can be assumed to be circular in shape. The cross-sectional area A_2 can be expressed using the pinhole radius.

Thus, the airflow through the pinhole, Q_{air} (mL/min), is proportional to the product of the cross-sectional area of the pinhole and the absolute inlet pressure. The water overflow rate, Q_{wof} (mL/min), is also proportional to the product of the right side of Eq. (2):

$$Q_{\text{wof}} \propto Q_{\text{air}} \propto k \pi r^2 \times P_{\text{abs}} \quad (2)$$

where k represents a coefficient; r represents the pinhole radius (μm); and P_{abs} represents the absolute pressure (P_{gauge} [343] + 101.3) (kPa).

The model curve was made using the above quadratic equation for approximating the relationship between the pinhole-associated water overflow and the actual pinhole size measured by scanning electron microscopy.

2.6. Leak value (L_v) measurement

The volume of water overflowing from the pinhole filter was converted to the L_v using a Planova™ Leak Tester (PLT-AM10, Asahi Kasei Medical, Co., Ltd., Tokyo, Japan). For filters with an effective surface area of 0.1, 1.0, and 4.0 m², the permeate side was filled with air-saturated water at 25 °C under ambient atmospheric pressure, and the leak test was performed using the PLT instrument according to the manufacturer's instructions (i.e., for BioEX filters, pressure: 343 kPa (3.43 bar, 49.7 psi); charge: 300 s; L_v defined as pressure increase, Pa/5 s). The PLT is designed to measure the water overflow attributable to airflow through a filter caused by diffusion from normal pores and bulk flow from pinholes. The increase in the pressure of the air chamber outside the filter is determined using a highly sensitive differential pressure sensor [31,32]. The relationship between water overflow rate and L_v was determined using various pinhole-containing and normal filters.

In the L_v model calculation, the amount of gas (provided by the water overflow rate) and the inner volume of the air in the PLT were substituted into the “ideal gas law”:

$$P = \frac{nRT}{V} \quad (3)$$

where P represents the absolute pressure of the gas; V represents the volume of the gas; n represents the quantity of the gas (measured in moles); R represents the ideal (or universal) gas

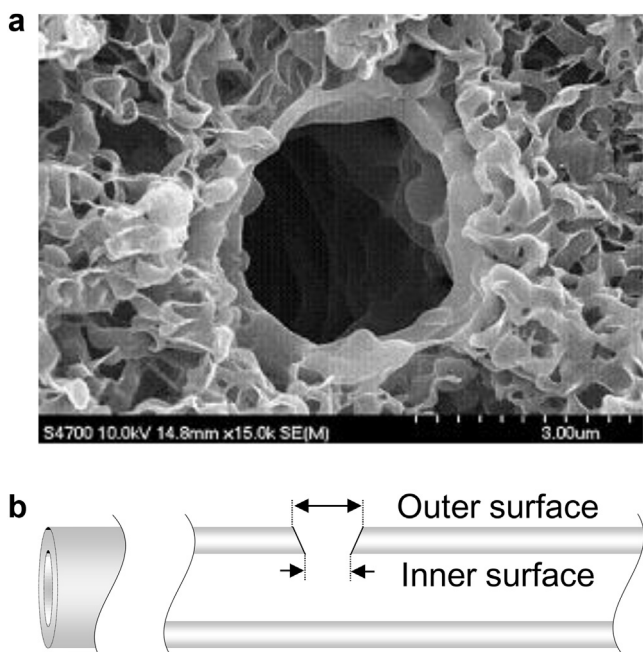


Fig. 1. (a) Pinhole (3.2 μm) on the inner surface of a hollow fiber, as observed by scanning electron microscopy. (b) Schematic representation of an artificially created pinhole on the surfaces of a Planova™ BioEX hollow fiber.

constant, $8.31 \text{ (L kPa K}^{-1} \text{ mol}^{-1})$; and T represents the absolute temperature of the gas.

In determining the L_v using the PLT, “equivalent inner volume” refers to the total volume of any bulk air in the space between the filter permeate side and the differential pressure sensor, including air in the tube line and filter housing. The equivalent inner volume would be underestimated. In case of an extremely large air volume from a large pinhole could not be held in the filter housing, and thus, a portion of the air would escape before the L_v measurement step. This would lead to a higher L_v than the model calculation.

2.7. Determining the size of the smallest recognizable pinhole

Here, we describe how the size of the smallest recognizable pinhole was determined under the standard L_v acceptance criteria. Fig. 2 shows the relationship between L_v value deviation, standard acceptance criteria, and smallest recognizable pinhole size. In this study, we set the standard acceptance criterion to 4 SDs of the mean value for normal, non-defective filters. This criterion gives a probability of a false failure (i.e., a non-defective filter is misjudged as being defective) of approximately 3/100,000. Because a pinhole filter is identical to a normal filter except for the pinhole defect, we assume that the SD of a pinhole filter L_v should be the same as that of a normal filter.

The probability of a false pass (i.e., a defective pinhole filter is misjudged as non-defective) was set as follows. Considering the discrimination of false pass and false fail under same probability setting (defined as no overlap for normal-filter mean +4SD and pinhole-filter mean -4SD), the smallest size pinhole for which the entire mean ± 4 SD lies above the L_v cutoff was designated as the smallest recognizable pinhole. This value can be back-calculated using the pinhole-filter L_v . The “smallest pinhole to fail” the leakage test is considered to be the “largest pinhole size to pass” the leakage test, defining the boundary between filters recognized as normal (pass) or having a pinhole (fail).

3. Results

3.1. Effect of harsh conditioning on pore-size distribution

Table 1 shows the virus removability of 0.001-m^2 Planova™ BioEX filters after exposure to harsh conditioning. Tests were conducted on four individual filters for each condition. All PPV LRV

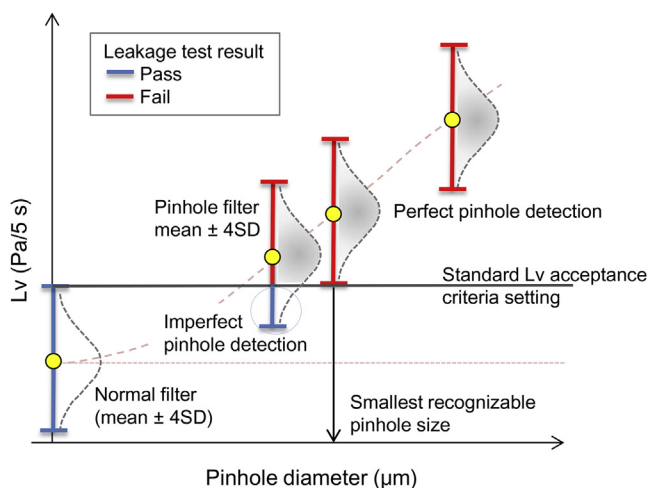


Fig. 2. Schematic illustration of the relationship between leak value (L_v) deviation, standard acceptance criteria, and size of smallest recognizable pinhole.

Table 1
Virus removability after exposure of filter to harsh conditions.

Harsh stress conditioning (12 h at 392 kPa ^a)		PPV LRV ^b (n = 4)
pH	Temperature (°C)	
Control ^c		≥5.17
		≥5.50
		≥5.50
		≥5.17
2 ^d	40	≥5.00
		≥5.50
		≥5.50
		≥5.17
10 ^e	40	≥5.00
		≥5.50
		≥5.50
		≥5.17

^a 392 kPa (3.92 bar, 56.9 psi).

^b PPV LRV: porcine parvovirus logarithmic reduction value.

^c Control filters were used without any harsh conditioning.

^d Hydrochloric acid aqueous solution.

^e Sodium hydroxide aqueous solution.

data exceeded the detection limit ($\geq 5.00 \sim \geq 5.50$), demonstrating that harsh conditioning of the filters before virus challenge did not affect virus removability.

Larger area Planova™ BioEX filters (0.01 m^2) were also exposed to the same harsh conditioning. Each of these filters was then used to filter solutions of colloidal gold. The control filters showed gold particle LRVs of 2.23 and 2.19, whereas the LRVs of filters subjected to low- and high-pH harsh conditioning were 2.25 and 2.26 and 2.30 and 2.37, respectively (Table 2). These LRV data were similar and did not exceed the upper detection limit of the LRV assay, indicating that they are quantitatively comparable.

3.2. Water overflow rate and pinhole size

The water overflow rate attributable to pinholes was plotted as a function of pinhole diameter (Fig. 3). The experimentally observed pinhole-attributable portion of the water overflow value was proportional to the square of the pinhole diameter.

3.3. L_v determinations for various filters

Fig. 4 shows the relationship between L_v and water overflow rate. Normal filters showed a range in inherent L_v caused by air diffusing through the normal pores, in accordance with the difference in the total effective surface area. The L_v s of pinhole filters

Table 2
Gold particle removability, confirmation of no shift in proper pore size distribution after exposure of filter to harsh conditions.

Harsh stress conditioning (12 h at 392 kPa ^a)		Gold particle LRV ^b (n = 2)
pH	Temperature (°C)	
Control ^c		2.23
		2.19
2 ^d	40	2.25
		2.26
10 ^e	40	2.30
		2.37

^a 392 kPa (3.92 bar, 56.9 psi).

^b Gold particle LRV: gold particle logarithmic reduction value.

^c Control filters were used without any harsh conditioning.

^d Hydrochloric acid aqueous solution.

^e Sodium hydroxide aqueous solution.

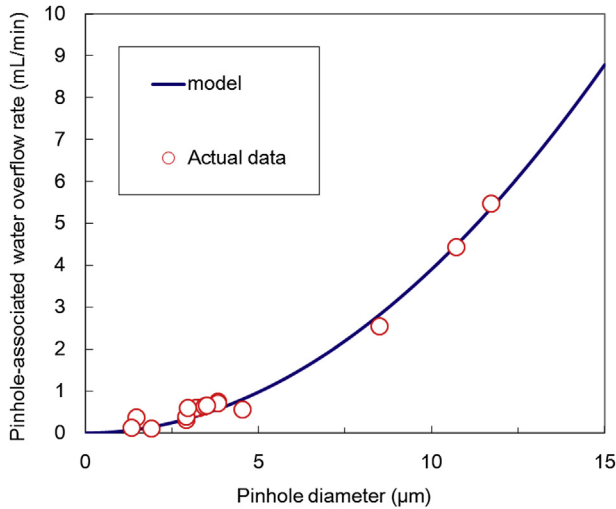


Fig. 3. Correlation between water overflow rate attributable to the pinhole and pinhole size. The pinhole-associated water overflow rate (mL/min) was calculated by subtracting the water overflow rate of a normal (intact) filter from the water overflow rate of a pinhole filter.

were larger than those of normal filters having the same effective surface area. Moreover, Lvs of several pinhole size spread wide on the curve. The real data showed an excellent correlation with the model calculation, regardless of the presence of a pinhole in the filter. Thus, the conversion of pinhole-attributable water overflow rate to Lv is quantitative.

3.4. Relationship between pinhole diameter and virus removal rate

The correlation between pinhole diameter and virus removal rate was also investigated, and Fig. 5 summarizes the relationship between these parameters. The PPV LRV of points marked with an upward arrow was higher than the detection limit. Pinholes <2 µm had PPV LRVs ≥5.5. Viruses likely pass through the artificially generated micron-sized pinhole defect, but the permeate flow through the defect is too small compared with the overall permeate flow to measurably impact the LRV. For 0.1-m² Planova™ BioEX

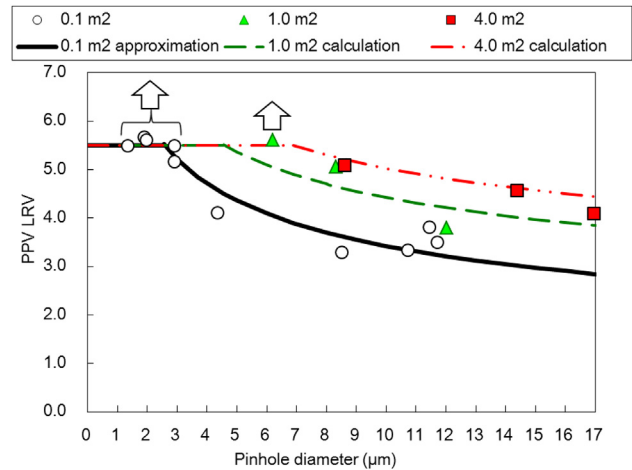


Fig. 5. Relationship between virus removal rate and pinhole diameter. The arrowhead means the value exceeded the logarithmic reduction value (LRV) upper detection limit. Open circles, 0.1-m² filter; closed green triangles, 1.0-m² filter; and closed red squares, 4.0-m² filter. The solid line indicates the curve fit (approximating a power function) for the 0.1-m² filter actual plot data. The dotted lines indicate extrapolation to the 1.0- and 4.0-m² filters using the above approximation.

filters, a decline in PPV LRV was observed beginning at around 3 µm, and the reduction in LRV increased in magnitude with increasing pinhole diameter. For filters with larger effective surface areas, the impact on PPV LRV was less than that for the 0.1-m² Planova™ BioEX filter. This is most clearly seen in Fig. 5 for pinholes between 8 and 9 µm, where the PPV LRV is 3.3 for a filter with an effective surface area of 0.1 m² and 5.0 for filters with effective surface areas of 1.0 and 4.0 m². Therefore, single pinhole defects have less of an impact on the LRV of filters with larger effective surface areas. The fitted curve (approximating a power function) for the 0.1-m² Planova™ BioEX filter actual plot data is indicated as a solid line. The data were then extrapolated to 1.0- and 4.0-m² Planova™ BioEX filters (broken lines) for modeling the PPV LRV. These extrapolations were based on the following assumption: under the same constant-pressure operating conditions, the number of virus particles that leak through the pinhole is the same and is independent of the filter's effective surface area. The total permeate volume increases with increasing effective surface area. Therefore, the concentration of virus in the permeate solution should decrease in an inverse proportional manner. Some actual data followed these lines. It is possible to evaluate the impact on virus removability by determining the size of the defect, in microns.

3.5. Normal-filter Lv deviation and standard acceptance criteria

Table 3 summarizes the mean and SD of the measured Lv for filters of each effective surface area. The end-user standard Lv

Table 3
Standard leak value (Lv) acceptance criteria for leakage test using the Planova leak tester.

Effective surface area (m ²)	Lv (Pa/5 s)		Standard Lv acceptance criterion ^b (Pa/5 s)
	Mean ^a	Standard deviation ^a	
0.1	6	3	≤18
1.0	153	24	≤249
4.0	463	60	≤703

^a From data on intact filters (no pinholes).
^b Standard Lv acceptance criterion determined by adding four standard deviations (4SD) to the mean value for normal, non-defective filters.

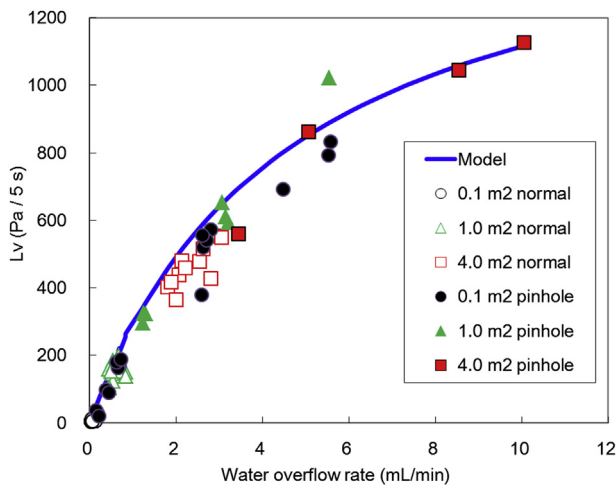


Fig. 4. Correlation between leak value (Lv) and water overflow rate. Circles, 0.1-m² filter; triangles, 1.0-m² filter; squares, 4.0-m² filter. Open symbols indicate normal filters, and closed symbols indicate pinhole filters. Curve indicates the model calculation for filter Lv as a function of water overflow rate.

acceptance criteria for 0.1-, 1.0-, and 4.0-m² Planova™ BioEX filters were ≤18, ≤249, and ≤703 Pa/5 s, respectively. The process for determining the standard acceptance criteria was described in the Material and methods section and summarized in Fig. 2.

3.6. Size of the smallest recognizable pinhole in the leakage test

Fig. 2 explains our approach for setting the standard acceptance criteria and determining the smallest recognizable pinhole for the leakage test as an end-user IT. Fig. 6a–c show the size of the smallest recognizable pinhole for 0.1-, 1.0-, and 4.0-m² Planova™ BioEX filters under each standard acceptance criterion, respectively. The calculated model curve in Fig. 6a shows the predicted mean Lv for pinholes of various diameters in a 0.1-m² Planova™ BioEX filter. The predicted mean Lv is based on the correlation between the data depicted in Figs. 3 and 4. The mean Lv +4SD (i.e., the standard acceptance criterion) for the non-defective filter was 18 Pa/5 s (Table 3). The size of the smallest recognizable pinhole for the leakage test is thus estimated at approximately 1.4 μm. This pinhole diameter is indicated by an arrowhead in Fig. 6a.

Similar analyses were performed for 1.0- and 4.0-m² Planova™ BioEX filters, returning values of approximately 4.6 and 13.1 μm, respectively (Fig. 6b and c). As shown in Fig. 6b, pinholes much larger than the smallest recognizable pinhole size fit the model calculation poorly. However, this phenomenon would only occur with a pinhole that is very large relative to the smallest

recognizable pinhole size described in section 2.6 and should not affect the smallest recognizable pinhole size estimation. The size of the smallest recognizable pinhole would thus be predicted to increase with increasing effective surface area.

3.7. Estimation of the impact of smallest recognizable pinhole size on virus removability

To estimate how the size of the smallest recognizable (in other words, the “largest allowable”) pinhole impacts virus removability, each predicted smallest recognizable pinhole diameter was evaluated according to the virus removal relationship shown in Fig. 5. The detection of gross defects using this IT can be correlated with the filter’s virus clearance. In the cases of 0.1- and 1.0-m² effective surface area filters having the largest allowable pinhole size, the PPV LRV was predicted to exceed the upper detection limit (≥5.5). In the case of a 4.0-m² filter with a pinhole, a slight decline in PPV LRV was predicted, but the PPV LRV still remained high (4.7). Table 4 summarizes the estimated PPV LRV for each predicted smallest recognizable pinhole diameter for each effective surface area.

4. Discussion

In this work, we demonstrated that pinhole defects, at or below a certain size for each effective surface area, have no significant

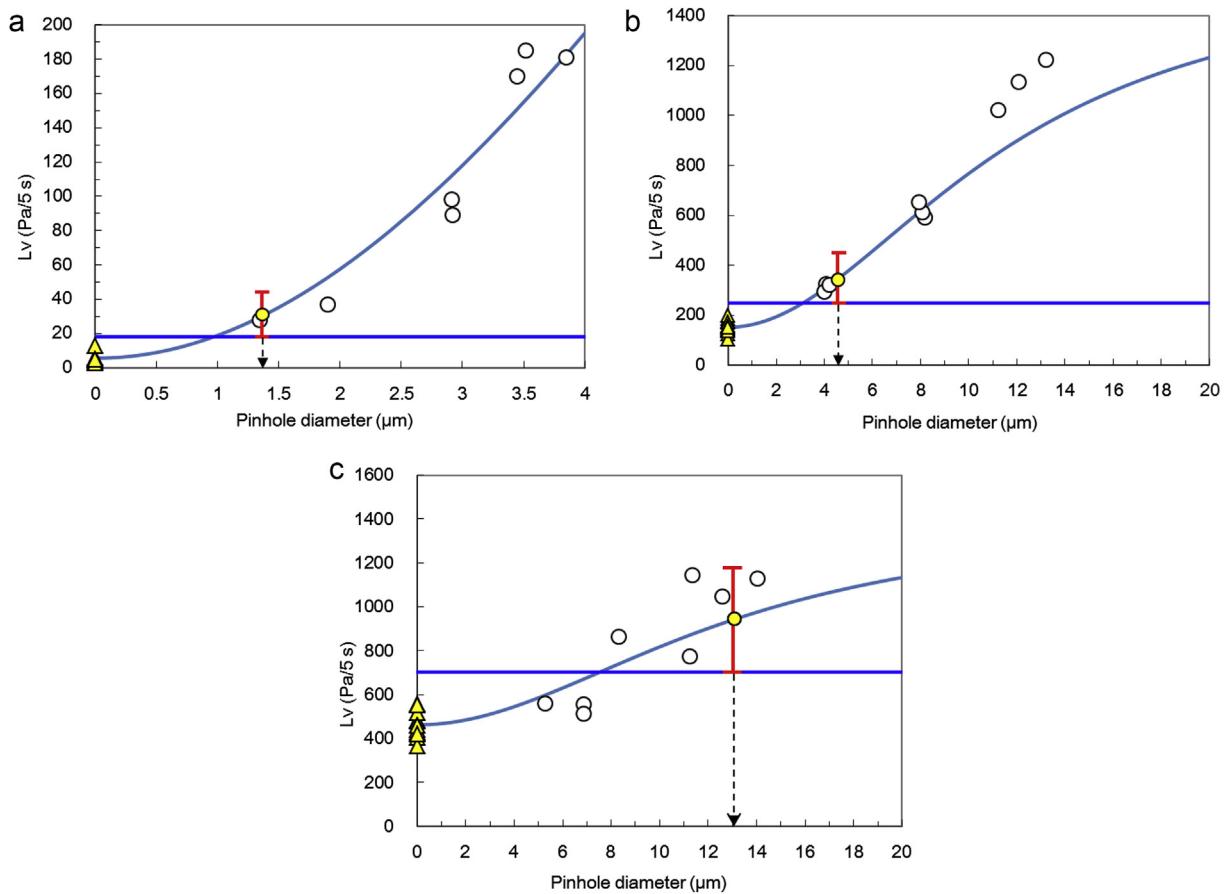


Fig. 6. (a) Smallest recognizable pinhole size estimated based on the standard acceptance criterion for 0.1-m² Planova™ BioEX filters. Curve indicates the model calculation for filter leak value (Lv) as a function of pinhole diameter. Bar indicates ±4SD of the filter Lv. Horizontal line indicates standard acceptance criterion setting. Closed yellow triangles indicate normal filter data, and open circles indicate pinhole filter data. Closed yellow circles indicate predicted Lv and pinhole diameter. (b) Smallest recognizable pinhole size estimated based on the standard acceptance criterion for 1.0 m² Planova™ BioEX filters. (c) Smallest recognizable pinhole size estimated based on the standard acceptance criterion for 4.0-m² Planova™ BioEX filters.

Table 4
Standard leak value (Lv) acceptance criteria and estimation of the impact on virus removability.

Effective surface area (m ²)	Standard Lv acceptance criterion (Pa/5 s)	Smallest recognizable pinhole size (diameter, μm) ^a	Estimated PPV LRV ^b
0.1	≤18	1.4	≥5.5
1.0	≤249	4.6	≥5.5
4.0	≤703	13.1	4.7

^a The “smallest recognizable pinhole size” for the leakage test is also considered the “largest pinhole size to pass” the leakage test.

^b The PPV LRV of filters considered intact is ≥5.5 (PPV LRV: porcine parvovirus logarithmic reduction value).

impact on virus LRV. We used the water overflow rate to determine the pinhole size. The model curve was constructed using a quadratic equation for approximating the relationship between the pinhole-attributable portion of the water overflow and the actual pinhole size as measured by scanning electron microscopy. It is well known that for virus filters with a normal pore size distribution and pore size (on the order of less than approximately 100 nm) that are pre-wetted with water, the BP value in water exceeds approximately 300 psi (2 MPa). At pressures below the BP, air will migrate though the liquid (water) within the pore structure of a wetted filter, in accordance with Fick's law of diffusion [10,16,19]. In contrast, in the case of a filter with a micron-sized pinhole defect, the air can pass through the pinhole as bulk flow, even at pressures below the integral filter BP. Moreover, an inlet pressure of 343 kPa (3.43 bar, 49.7 psi) is significantly higher than the downstream (permeate side of the filter) pressure, so the airflow through any pinhole can be considered choked flow (i.e., critical flow) [22,30]. Under these conditions, the airflow from a single pinhole defect can be modeled as a critical flow nozzle for air (see Material and methods section; Eq. (1); adapted from Ref. [30], section 10–19 “Critical flow nozzle,” equation (10–33)).

Fig. 3 shows the model curve fit to the pinhole-attributable portion of the actual water overflow. These phenomena satisfied the critical flow nozzle for air model described above and in the Material and methods section. Moreover, the airflow rate and water overflow rate are proportional to the pinhole cross-sectional area (Material and methods section; Eq. (2)). Under the experimental conditions used in this study (343 kPa [3.43 bar, 49.7 psi], 25 °C), the relationship between pinhole diameter, D (μm), and water overflow, Q_{wof} (mL/min), is approximated and can be expressed as follows:

$$D = \sqrt{\frac{Q_{wof}}{0.03905}} \quad (4)$$

Fig. 4 shows the correlation between observed Lv and water overflow rate. The pinhole Lv data included data for filters with various pinhole sizes (including unrecognizable pinholes). Therefore, the Lv of “normal filters” for different filter sizes are clustered, whereas for the same filter sizes, the values for filters with pinholes are distributed over a wide range. For some filters with unrecognized pinholes, the Lv was close to the normal value.

Two types of defects may affect the removal capability of virus filters: 1) improper pore size distribution, and 2) gross damage, such as pinholes. These parameters should be evaluated by the end-user for proper pore-size distribution and absence of gross defects [10]. As prior to shipment, Planova™ BioEX filters are inspected by the manufacturer for proper pore-size distribution using a new pressure hold test, and the absence of defects is confirmed using an air/water diffusion-based leakage test, the necessity of evaluating

pores size distribution and gross defects after shipment and usage of the Planova™ BioEX filters by the end user have to be addressed.

Once a filter is shipped, no shift in pore-size distribution should occur under usage conditions if the filter has sufficient mechanical strength. PVDF hollow fibers reportedly exhibit mechanical performance superior to that of polysulfone membranes [15]. The cellulose membrane material used to make standard Planova™ virus filters has lower mechanical strength than PVDF, explaining why the typical working pressure for these filters is limited to 98 kPa (0.98 bar, 14.2 psi), lower than that of Planova™ BioEX filters [18]. To confirm the superior mechanical and chemical resistance properties of the BioEX filters, filters were subjected to harsh conditioning by filtration of either a low- or high-pH solution at high temperature under a filtration pressure of 392 kPa (3.92 bar, 56.9 psi) for 12 h, conditions that exceed the typical operating conditions (i.e., operating pressure of 196–343 kPa [1.96–3.43 bar, 28.4–49.7 psi]; operating pH of 4–8; operating temperature of 8–25 °C). All LRVs exceeded the upper detection limit in the virus-spiking experiments (Table 1). These results are even more conclusive after consideration of the complementary quantitative GPT data, which confirmed that harsh conditioning does not lead to a shift in the pore size distribution (Table 2). The BioEX filters showed durable PPV LRV and GPT LRV responses even after harsh conditioning (Tables 1 and 2), indicating the absence of a shift in the pore-size distribution of the hollow fibers and that there is no risk that virus removal capabilities will be compromised under typical end-user filtration conditions. Therefore, end-users might not need to check for proper pore-size distribution using methods such as the GPT.

Several reports have discussed the complexation of virus particles by immunoglobulins [33,34]. Planova™ 35N (mean pore size: 35 nm) were used in our virus-spiking experiments as a pre-filter for preparing single dispersed PPV particles in polyclonal human IgG solution. We confirmed that the virus titers were nearly identical (within 0.2-log) before and after the Planova 35N pre-filtration and that the titers did not change over time after pre-filtration. These data indicate that complexation or aggregation of PPV particles was unlikely under our experimental conditions.

It is important to also consider the risk of underestimation of the virus LRV decline. If a normal filter contains an undetectable pinhole and virus breakthrough occurs, the LRV decline of pinhole filter will be underestimated. We used a small virus (PPV) to evaluate the effectiveness of virus removability. Small viruses can pass through an undetectable pinhole more readily than large viruses. In our study, the LRV of the normal filter was set to the upper detection limit. Thus, there was no risk of underestimation.

In the present study, a large volume (105 L/m²) was filtered through the harshly conditioned filter not exhibiting any detectable pinhole. Although a slight flux decay was observed under this filtration condition (data not shown), there were no differences in PPV LRV (Table 1). Due to experimental limitations, we used an early stage of the filtration sample (2–3 L/m²) in our pinhole filter PPV challenge experiment; we did not observe any flux decay throughout the filtration. Therefore, we trust that our results were appropriate for accurate evaluation of the impact of pinhole gross defects on the PPV LRV, free of an effect of flux decay. However, during nanofiltration of biological products in a production setting, a filter may become blocked by proteins, thus lowering the permeate flow rate. On the other hand, the rate of flow through a recognizable pinhole is likely to remain the same, even when the overall permeation rate decreases. Therefore, a large flux decay during filtration might exacerbate the decline in the LRV for a pinhole filter. Users should thus select the filtration conditions keeping the degree of filtration flux decay as small as possible.

The purpose of the leakage test is to detect gross filter defects, such as broken fibers and pinholes that may have occurred as a result of damage during shipping or filtration. Pinholes can be detected by the BP method when evaluating a filter's compliance with IT acceptance criteria by using the relationship between the IT value and the virus LRV; however, the IT value must be obtained quantitatively from a normal-integrity filter (without pinhole). If the IT value of the normal filter were obtained using the water-wetted BP method, in the case of a virus filter with a 20-nm normal pore size, it would be necessary to pressurize the filter to 14.4 MPa (when substituting $k \cos \theta = 1$, water surface tension = 71.96 dyne/cm in the Young–Laplace equation; BP method principle). However, such an extremely high pressure could disrupt the filter membrane structure and damage the filter housing. A pressure of this magnitude also far exceeds the recommended filtration pressure (i.e., 343 kPa [3.43 bar, 49.7 psi]). An organic solvent with a lower surface tension might reduce the BP pressure, but this would necessitate solvent change. Thus, this method is not suitable for pre-use user integrity testing.

A simple leakage visual test can be conducted under the lower pressure of the membrane BP, and leaks can be detected visually as a steady stream of air bubbles on the permeate side of the filter. This type of test is suitable for detecting pinholes in filters with a relatively small effective surface area. However, sensory evaluations such as this are not easy to standardize and are thus burdensome for operators in production of biologicals. Generally, forward/diffusive flow is considered to correlate with virus retention. Here, we demonstrated that the PLT-determined L_v can be correlated with Planova™ BioEX filter virus removal capability, as discussed further below.

For integrity testing, it is necessary to consider the worst-case situation for the observed L_v . We used filters containing a single pinhole to model the presence of a gross defect. The gas flow rate should be the same for filters of the same total cross-sectional area, regardless of the number of pinholes. Thus, the L_v should be the same for filters with a single large pinhole defect and filters with multiple smaller pinhole defects having the same total cross-sectional area. On the other hand, the rate of liquid flowing through a pinhole is correlated with the biquadrate of the pinhole diameter. Virus particles pass through the defect along with proteins in solution. This means that virus particles behave as a liquid. It has been reported that particle-containing liquid flowing through a filter defect can be modeled according to Hagen–Poiseuille flow [21,23,30]. Thus, a single large pinhole has a larger effect on the flow of a virus-containing solution than the sum of multiple small pinholes. A single large pinhole could be considered as having a greater impact on virus LRV than multiple small pinholes, assuming the same L_v is observed in both cases. Therefore, it is reasonable to use filters containing a single pinhole defect for experiments to model worst-case effects of gross defects. Similar considerations have been reported for laminar liquid flow [24] and turbulent-channel and orifice liquid flow models [22]. In addition, decreases in flow rate toward the end of the filtration process could be attributed to adsorption of protein onto the filter surface, which would be expected to occur uniformly over the entire surface, regardless of pore shape. Under such conditions, small pinholes (including those that are undetectable) may clog faster than large pinholes. From this point of view, a single large pinhole would be considered the worst-case scenario.

Because the filter L_v reflects the sum of the air diffusion through wetted normal pores and the bulk airflow from pinhole defects, it might be harder to discriminate very small defects in the case of filters having larger effective surface areas. We therefore must address the sensitivity and limitations of the leakage test standard

acceptance criteria. The PLT is designed to achieve sufficient sensitivity to detect small leaks. The PLT is equipped with a sensitive differential pressure sensor with an inner chamber of low air volume. To obtain stable results, the filter's permeate side is filled with air-saturated water [31,32]. However, it is known that the results of forward/diffusive flow tests can be affected by a variety of conditions. Therefore, it is important to use appropriate measurement conditions, as described in the manufacturer's instructions. In principle, other IT instruments could be employed to evaluate similar pinhole leaks, but the conditions and criteria used should be carefully chosen and individually confirmed.

The basis for setting the standard L_v acceptance criteria takes into account the effective surface area of the filter (Fig. 2). The size of the smallest recognizable pinhole depends on the filter type (i.e., a larger effective surface area filter requires a larger pinhole size for recognition) (Fig. 6a–c). In contrast, the impact of the same size pinhole defect on the PPV LRV is predicted to diminish as the filter's effective surface area increases (Fig. 5). Estimations of the impact on virus removability for each type of filter are summarized in Table 4. Whereas the decline in PPV LRV was small for the largest filter (4.0 m²), the PPV LRV for filters of all sizes was ≥ 4.7 . However, the possibility of variation in the PPV LRV (generally ± 0.5 log) should also be considered.

The World Health Organization has reported that for human plasma products, a robust, effective, reliable process should be able to remove or inactivate a substantial number of virus particles (typically 4 logs or more), be easy to model convincingly, and be relatively insensitive to changes in process conditions [3]. Also, a document from the European Medicine Agency mentions that viral reductions on the order of 4 logs or more are indicative of clear inactivation/removal effect of a particular test virus evaluated [5]. The extent of targeted virus removal may vary depending upon specific medicinal products and operating procedures, as part of a risk assessment exercise. Acceptance criteria would have to be validated for each production process at the end-user's site.

In conclusion, under our experimental conditions, suitable virus removal was achieved for filters that passed the leakage test. The rate of detrimental shifts in pore-size distribution is negligible under normal filtration conditions for PVDF hollow fibers. The IT performed by the end user needs to cover only damage that may have occurred post shipping or handling, such as tears, broken fibers, or pinholes. Therefore, the leakage test and standard acceptance criteria described here are sensitive enough to be employed as the only end-user IT for Planova™ BioEX filters.

Acknowledgments

The authors thank L.P.S. Works Co., Ltd. for their laser processing of pinhole fibers. The authors thank Dr. Marcus Inouye, Dr. Masayasu Takahara, Mr. Tomo Miyabayashi, and Mr. Fujiharu Nagoya for their valuable suggestions, Mr. Nobufumi Kawano, Mr. Kazuya Kobayashi, and Dr. Kouichirou Yanagida for their skillful experimental assistance, Ms. Linda Gudex for assistance in preparing the manuscript, and Dr. Thierry Burnouf for his valuable discussions to improve the final manuscript.

Conflict of interest

All of the authors are employees of Asahi Kasei Medical and its related company.

References

- [1] Burnouf T. Modern plasma fractionation. *Transfus Med Rev* 2007;21:101–17.

- [2] Badrot A, Schuepp M, Green G. The contract biomanufacturing market outlook to 2017 outsourcing/manufacturing. Data Monitor Healthcare: Informa UK Ltd.; 2013.
- [3] World Health Organization. Guidelines on viral inactivation and removal procedures intended to assure the viral safety of human blood plasma products. WHO Tech Rep Ser 2004;924:150–224 (Annex 4).
- [4] ICH Harmonised Tripartite Guideline. Viral safety evaluation of biotechnology products derived from cell lines of human or animal origin Q5A(R1). 1999;Curr step 4 ver.
- [5] EMEA/CPMP/BWP. Note for guidance on virus validation studies: the design, contribution and interpretation of studies validating the inactivation and removal of viruses. EMEA/CPMP/BWP/268/95; 1996.
- [6] EMEA/CHMP/BWP. Guideline on virus safety evaluation of biotechnological investigational medicinal products. EMEA/CHMP/BWP/398498; 2009.
- [7] United States Food and Drug Administration (FDA) Center for Biologics Evaluation and research (CBER). Points to consider in the manufacture and testing of monoclonal antibody products for human use. Docket No. 94D-0259. 1997.
- [8] Velthove KJ, Over J, Abbink K, Janssen MP. Viral safety of human plasma-derived medicinal products: impact of regulation requirements. *Transfus Med Rev* 2013;27:179–83.
- [9] Burnouf T, Radosevich M. Nanofiltration of plasma-derived biopharmaceutical products. *Haemophilia* 2003;9:24–37.
- [10] Parenteral Drug Association (PDA). Virus filtration Technical report No. 41 (Revised 2008). PDA J Pharm Sci Technol Suppl 2008;62(S-4).
- [11] Korneyeva M, Rosenthal S. Virus removal by nanofiltration. *Methods Mol Biol* 2005;308:221–31.
- [12] Remington KM. Viral safety from process development through validation. IBC's training academy course, course handbook. IBC Lifescience; 2007.
- [13] Khayet M, Feng CY, Khulbe KC, Matsuura T. Preparation and characterization of polyvinylidene fluoride hollow fiber membranes for ultrafiltration. *Polymer* 2002;43:3879–90.
- [14] Asatekin A, Menniti A, Kang S, Elimelech M, Morgenroth E, Mayes AM. Anti-fouling nanofiltration membranes for membrane bioreactors from self-assembling graft copolymers. *J Membr Sci* 2006;285:81–9.
- [15] Zhang Q, Lu X, Zhao L. Preparation of polyvinylidene fluoride (PVDF) hollow fiber hemodialysis membranes. *Membranes* 2014;4:81–95.
- [16] Jornitz MW, Meltzer TH. Filtration handbook: integrity testing. Raleigh NC: Davis Horwood Inter. Pub., Ltd.; 2003.
- [17] Phillips MW, DiLeo AJ. A validatable porosimetric technique for verifying the integrity of virus-retentive membranes. *Biologicals* 1996;24:243–53.
- [18] Roberts PL, Feldman P, Crombie D, Walker C, Lowery K. Virus removal from factor IX by filtration: validation of the integrity test and effect of manufacturing process conditions. *Biologicals* 2010;38:303–10.
- [19] Parenteral Drug Association (PDA). Sterilizing filtration of liquids technical report No. 26 (revised 2008). PDA J Pharm Sci Technol Suppl 2008;62(S-5).
- [20] Lebleu N, Roques C, Aimar P, Causserand C. Effects of membrane alterations on bacterial retention. *J Membr Sci* 2010;348:56–65.
- [21] Antony A, Blackbeard J, Angles M, Leslie G. Non-microbial indicators for monitoring virus removal by ultrafiltration membranes. *J Membr Sci* 2014;454:193–9.
- [22] Dowd CJ. Multi-round virus filter integrity test sensitivity. *Biotechnol Bioeng* 2009;103:574–81.
- [23] Giglia S, Krishnan M. High sensitivity binary gas integrity test for membrane filters. *J Membr Sci* 2008;323:60–6.
- [24] Bolton G, Cormier J, Krishnan M, Lewnard J, Lutz H. Integrity testing of normal flow parvovirus filters using air-liquid based tests. *BioProcess J* 2006;5:50–5.
- [25] Hongo-Hirasaki T, Komuro M, Ide S. Effect of antibody solution conditions on filter performance for virus removal filter Planova 20N. *Biotechnol Prog* 2010;26:1080–7. <http://dx.doi.org/10.1002/btpr.415>.
- [26] Yanagida K. Method for producing parvovirus having high infectivity titer. World Intellectual Property Organization (WIPO), WO2014/080676 A1 2014-05-30.
- [27] Reed LJ, Muench H. A simple method of estimating fifty per cent endpoints. *Am J Hyg* 1938;27:493–7.
- [28] Hamasaki N, Ide S. Method for test on integrity of microporous membrane. World Intellectual Property Organization (WIPO), WO2008/111510 A1 2008-09-18.
- [29] Hamasaki N, Ide S. Method of testing integrity of microporous membrane. US patent application publication, number US2010/0096328 A1 2010.
- [30] Perry RH, editor. Perry's chemical engineer's handbook. 8th ed. McGraw-Hill; 2007 [sections 6-10, 6-23, and 10-19].
- [31] Fukada S, Itose T. Device and method for detecting leakage of filter film. World Intellectual Property Organization (WIPO), WO98/29184 A1 1998-07-09.
- [32] Fukada S, Itose T. Device and method for detecting leakage of filter film. US patent number 6065329 2000.
- [33] Omar A, Kempf C. Removal of neutralized model parvoviruses and enteroviruses in human IgG solutions by nanofiltration. *Transfusion* 2002;42(8):1005–10.
- [34] Kreil TR, Wieser A, Berting A, Spruth M, Medek C, Pölsler G, et al. Removal of small nonenveloped viruses by antibody-enhanced nanofiltration during the manufacture of plasma derivatives. *Transfusion* 2006;46(7):1143–51.